

# Coherent Patterning of Matter Waves with Subwavelength Localization

J. Mompart,<sup>1</sup> V. Ahufinger,<sup>1,2</sup> and G. Birkl.<sup>3</sup>

<sup>1</sup>*Departament de Física, Universitat Autònoma de Barcelona, 08193 Bellaterra, Spain*

<sup>2</sup>*ICREA - Institució Catalana de Recerca i Estudis Avançats, Barcelona, Spain and*

<sup>3</sup>*Institut für Angewandte Physik, Technische Universität Darmstadt, Schlossgartenstraße 7, 64289 Darmstadt, Germany*

(Dated: May 5, 2019)

We introduce the Subwavelength Localization via Adiabatic Passage (SLAP) technique to coherently achieve state-selective patterning and addressing of matter waves. The SLAP technique consists in coupling two partially overlapping and spatially structured laser fields to three internal levels of the matter wave yielding state-selective localization at those positions where the adiabatic passage process does not occur. We show that by means of this technique matter wave localization down to the single nanometer can be achieved. We analyze in detail the potential implementation of the SLAP technique for nano-lithography with an atomic beam of metastable  $\text{Ne}^*$  and for coherent patterning of a two-component  $^{87}\text{Rb}$  Bose-Einstein condensate.

PACS numbers: 42.50.St, 42.50.Gy, 42.82.Cr

The highly controlled manipulation of atomic matter waves has proven to be an exciting field of research in recent years. Specially, research in Bose-Einstein condensation (BEC), Fermi quantum degeneracy, and quantum information processing with ultracold atoms has achieved tremendous advances. Future progress in this field will strongly profit from optical addressability, localization, and patterning of atomic systems with a resolution not limited by the wavelength of the radiation involved. Important examples are site-specific addressing and patterning of BECs in optical lattices [1] and atom lithography with the highest possible spatial resolution [2].

Recently, there have been several proposals for sub-wavelength atom localization based on the interaction of three-level atoms with light having a space-dependent amplitude distribution, mainly standing wave (SW) fields [3, 4, 5, 6, 7, 8]. In all these proposals a spatially modulated dark state is created by means of either electromagnetically induced transparency (EIT) or coherent population trapping (CPT) [9]. In fact, a proof-of-principle experiment based on the CPT technique reported intensity patterns in the transmission of a probe field presenting subwavelength spatial resolution [10]. Significant for the present work, the CPT technique with a SW control field produces atom localization in one of the ground states with a spatial fringe pattern resembling that of a Fabry-Perot resonator with cavity finesse given by the ratio  $\mathcal{R}$  between the control and probe field intensities [6].

In this letter, we propose a state-selective atom localization and patterning scheme based on Stimulated Raman Adiabatic Passage (STIRAP) [11, 12] that, compared to the CPT based techniques, presents several important advantages: (i) it produces 'super-localization', i.e., narrower localization than that expected from the CPT-finesse parameter  $\mathcal{R}$ ; (ii) it is a fully coherent process that does not rely on spontaneous emission to the dark state and, therefore, it can be applied to open three-level systems and to BECs; (iii) the localized state does

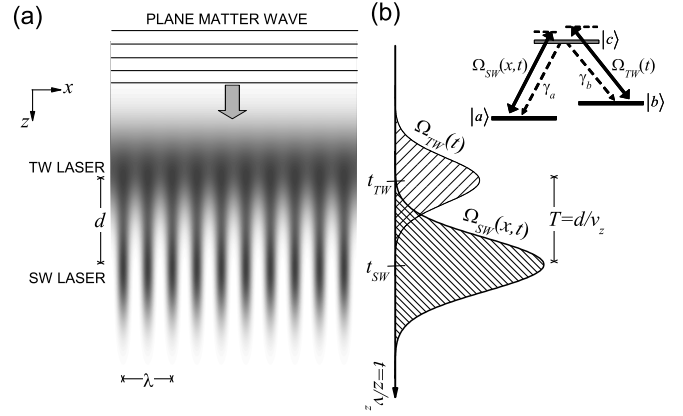


FIG. 1: (a) Schematics of the SLAP technique: A plane matter wave propagates consecutively through a TW and a partially overlapping SW laser field either in space (as shown here) or in time. (b) Three-level atomic system and Gaussian temporal profiles of the Rabi frequencies  $\Omega_{TW}(t)$  and  $\Omega_{SW}(x,t)$ .  $\gamma_a$  and  $\gamma_b$  account for the spontaneous emission decay rates of the corresponding transition.

not suffer from recoil induced broadening and, therefore, the Raman-Nath approximation holds [13], and, finally, (iv) it is robust under uncontrolled variations of the system parameters, e.g., intensity fluctuations of the laser fields. We describe here the main features of this Subwavelength Localization via Adiabatic Passage (SLAP) technique, as well as its potential implementation in nano-lithography with a metastable  $\text{Ne}^*$  matter wave and in patterning of a  $^{87}\text{Rb}$ -BEC. Note that STIRAP without the spatial localization feature introduced here has been proposed [14] and recently experimentally demonstrated [15] for the transition from an atomic to a molecular BEC and for the optical control of the internal and external angular momenta of an extended BEC [16].

The schematics of the SLAP technique are shown in Fig. 1. A plane matter wave formed by three-level atoms

in a  $\Lambda$ -type configuration propagates at a velocity  $v_z$  through two partially overlapping laser fields: the traveling wave (TW) couples the  $|c\rangle \leftrightarrow |b\rangle$  transition with a Rabi frequency  $\Omega_{TW}(t) = \Omega_{TW0} \exp(-(t - t_{TW})^2/\sigma_{TW}^2)$  and the SW couples the  $|c\rangle \leftrightarrow |a\rangle$  transition with a Rabi frequency  $\Omega_{SW}(x, t) = \Omega_{SW0} \sin kx \exp(-(t - t_{SW})^2/\sigma_{SW}^2)$ .  $k = 2\pi/\lambda$  is the SW field wave number and  $T = t_{SW} - t_{TW} = d/v_z$  the characteristic STIRAP time with  $d$  the spatial separation between the centers of the two laser beams.  $\Delta_{TW} = \omega_{TW} - \omega_{cb}$  ( $\Delta_{SW} = \omega_{SW} - \omega_{ca}$ ) is the single-photon detuning between the TW (SW) field and the corresponding transition.  $\gamma_a$  ( $\gamma_b$ ) is the spontaneous emission decay rate from  $|c\rangle$  to  $|a\rangle$  (from  $|c\rangle$  to  $|b\rangle$ ).

Under the two-photon resonance condition  $\Delta_{TW} = \Delta_{SW}$ , one of the position-dependent energy eigenstates of the  $\Lambda$ -type three-level system is the so-called dark state  $|D(x, t)\rangle = \cos\theta(x, t)|a\rangle - \sin\theta(x, t)|b\rangle$  where  $\tan\theta(x, t) = \Omega_{SW}(x, t)/\Omega_{TW}(t)$ . STIRAP [11] consists in following this energy eigenstate from  $|\psi_{in}\rangle = |a\rangle$  to  $|\psi_{out}\rangle = |b\rangle$  smoothly changing  $\theta$  from  $0^0$  to  $90^0$  by means of two partially overlapping laser fields as in the counter-intuitive sequence of Fig. 1. To keep the system in the energy eigenstate, the previous process must be performed fulfilling the 'global' adiabaticity condition [11]:

$$\Omega_{SW0}^2 \sin^2 kx + \Omega_{TW0}^2 > \left(\frac{A}{T}\right)^2 \quad (1)$$

where  $A$  is a dimensionless constant that for optimal Gaussian profiles and overlapping times takes values around 10 [12].

In the SLAP technique, we assume that the matter wave has been initially prepared, by means of e.g., optical pumping, into the internal state  $|a\rangle$ . Then, those atoms crossing the nodes of the SW remain in state  $|a\rangle$  while those interacting with both fields through the STIRAP process are transferred to state  $|b\rangle$ . Therefore, an intense SW field should produce sharp peaks on the spatial population distribution of state  $|a\rangle$  at its nodes. From Eq. (1) and assuming  $A > T\Omega_{TW0}$ , the FWHM of these peaks is given by:

$$(\Delta x)_{\text{SLAP}} = (\Delta x)_{\text{CPT}} \frac{1}{2} \sqrt{\left(\frac{A}{T\Omega_{TW0}}\right)^2 - 1} \quad (2)$$

where  $(\Delta x)_{\text{CPT}} = 2/k\sqrt{\mathcal{R}}$  with  $\mathcal{R} \equiv \Omega_{SW0}^2/\Omega_{TW0}^2$  is the FWHM of the peaks in the Fabry-Perot type localization that would be attained by means of the CPT technique [6]. Therefore, for

$$T\Omega_{TW0} = \frac{d}{v_z} \Omega_{TW0} > \frac{A}{\sqrt{5}} \quad (3)$$

the 'super-localization' regime which we define by  $(\Delta x)_{\text{SLAP}} < (\Delta x)_{\text{CPT}}$  is reached. Note that for  $A = 10$  corresponding to optimal parameter values [12], condition (3) reads  $T\Omega_{TW0} > 4.5$ .

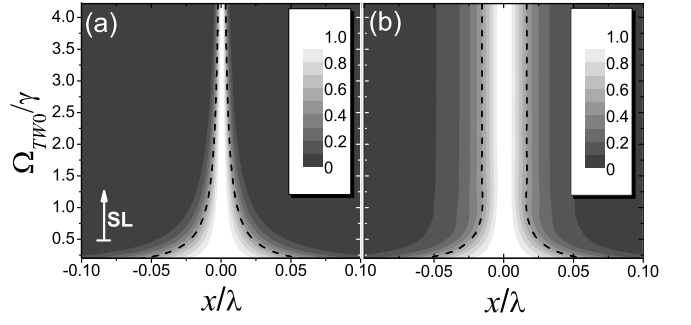


FIG. 2: Population distribution of state  $|a\rangle$  after applying (a) the SLAP technique and (b) the CPT technique as a function of the amplitude of the TW Rabi frequency  $\Omega_{TW0}$  for  $\mathcal{R} = 100$ ,  $\gamma\sigma_{TW} = \gamma\sigma_{SW} = 5$ ,  $\Delta_{TW} = \Delta_{SW} = 0$ ,  $\gamma T = 10$  for the SLAP case, and  $\gamma T = 0$  for the CPT case. The horizontal separation between the dashed curves gives the FWHM of the corresponding localized structure. SL in (a) indicates the regime of 'super-localization' with  $(\Delta x)_{\text{SLAP}} < (\Delta x)_{\text{CPT}}$ .

Fig. 2 shows numerical simulations of the state selective localization process by integrating the corresponding density matrix equations for both the SLAP and the CPT techniques. In the CPT technique [6], subwavelength state-selective localization is obtained by reaching the steady-state through an optical-pumping process to the dark-state involving several cycles of laser excitation and spontaneous emission. In the setup of Fig. 1, the CPT process corresponds to  $T = 0$ ,  $\sigma_{TW} = \sigma_{SW}$  and  $\gamma\sigma_{TW} \gg 1$ , where we have assumed, for simplicity,  $\gamma_a = \gamma_b (\equiv \gamma)$ . For  $\mathcal{R} = 100$  and the rest of parameters given in the figure caption, Fig. 2(a) shows that for  $\Omega_{TW0} > 0.45\gamma$  the super-localization condition (3) is fulfilled and the SLAP technique yields better localization than the CPT technique, i.e.,  $(\Delta x)_{\text{SLAP}} < (\Delta x)_{\text{CPT}} \sim 0.032\lambda$ .

As a first implementation, we consider atom lithography based on substrates sensitive to the internal energy of metastable atoms [17]. For this purpose, we take a plane matter wave of metastable  $\text{Ne}^*$  whose initial internal level  $= 2p^53s(^3P_0)$  has an energy of 16.6 eV and thus high potential for surface damage. In fact,  $\text{Ne}^*$  is a prime candidate for coherent manipulation, since the STIRAP technique has been successfully reported with  $\text{Ne}^*$  [18] using the  $\Lambda$  scheme  $2p^53s(^3P_0) \leftrightarrow 2p^53p(^3P_1) \leftrightarrow 2p^53s(^3P_2)$  where the first and the last are long lived states (see Fig. 3(a)). However, here we are interested in applying the SLAP technique such that, away from the nodes of the SW, the initial state is adiabatically transferred to a fast decaying state in order to remove the corresponding high internal energy. Thus we consider the open three-level  $\Lambda$  scheme  $2p^53s(^3P_0) \leftrightarrow 2p^53p(^3P_1) \leftrightarrow 2p^53s(^3P_1)$  (depicted in Fig. 3(a)) with state  $2p^53s(^3P_1)$  decaying to the ground state at a rate of  $2\pi \times 7.58 \cdot 10^6 \text{ s}^{-1}$ . Fig. 3(b) shows subwavelength atom localization in state  $2p^53s(^3P_0)$  (solid curve) around a node of the SW (period of 308.2 nm) after the application of the SLAP tech-

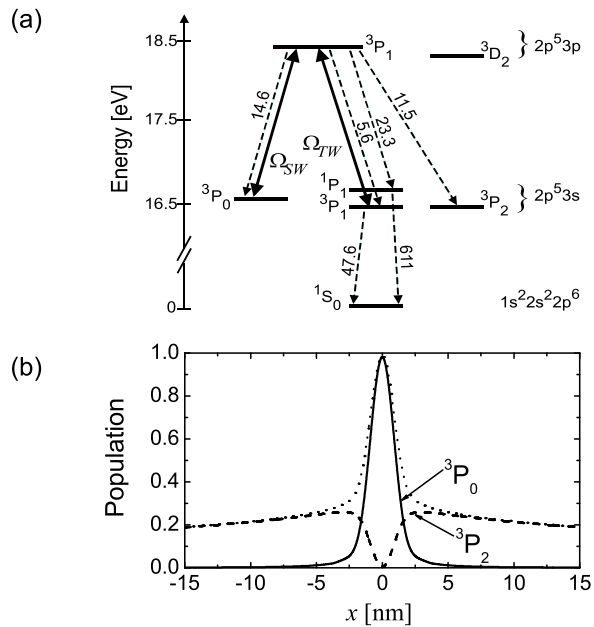


FIG. 3: SLAP technique for a  $\text{Ne}^*$  matter wave: (a) Relevant energy levels and Einstein A coefficients (in units of  $10^6 \text{ s}^{-1}$ ) for  $\text{Ne}^*$ . The TW field at  $\lambda_{TW} = 603.0 \text{ nm}$  couples transition  $2p^5 3s(^3P_1) \leftrightarrow 2p^5 3p(^3P_1)$  while the SW at  $\lambda_{SW} = 616.4 \text{ nm}$  couples  $2p^5 3s(^3P_0) \leftrightarrow 2p^5 3p(^3P_1)$ . (b) Final spatial population distribution around a node of the SW for state  $2p^5 3s(^3P_0)$  (solid curve),  $2p^5 3s(^3P_2)$  (dashed curve), and total high-energy state population (dotted curve). Parameters:  $v_z = 500 \text{ m/s}$ ,  $d = 100 \mu\text{m}$ ,  $\sigma_{TW} = \sigma_{SW} = 100 \text{ ns}$ ,  $\mathcal{R} = 400$ ,  $\Omega_{TW0} = 2\pi \times 1.6 \cdot 10^7 \text{ s}^{-1}$ , and  $\Delta_{TW} = \Delta_{SW} = 0$ .

nique for  $\mathcal{R} = 400$  and the other parameters given in the figure caption. Although part of the population (dashed curve) is diabatically transferred to the high energy state  $2p^5 3s(^3P_2)$  with lifetime  $\tau = 14.73 \text{ s}$  [19], this population could be efficiently pumped to the ground state via  $2p^5 3p(^3D_2)$  with an extra laser field. Thus, localization of the high-energy state with a FWHM of only a few nm can be achieved (solid line).

As an important feature of the SLAP technique, the localized state  $|a\rangle$  does not interact with the light fields at any time and therefore does not suffer from recoil induced broadening, which implies that the Raman-Nath approximation perfectly applies [13]. In this situation, the transversal velocity spread of the initial matter wave determines the ultimate resolution limit of the SLAP technique. Taking  $\overline{\Delta v_x}$  as the rms transversal velocity spread, the limit  $T\overline{\Delta v_x} \ll (\Delta x)_{\text{SLAP}}$  corresponds to  $\overline{\Delta v_x}/v_z \ll (\Delta x)_{\text{SLAP}}/d$ . Thus, for typical parameters,  $v_z = 500 \text{ m/s}$ ,  $\overline{\Delta v_x} = 5 \text{ cm/s}$ , and  $d = 20 \mu\text{m}$ , localization down to single nm can be achieved. As given by the Heisenberg uncertainty principle, strong atom localization should also result in the appearance of high momentum components [6]. For the results shown in Fig. 3(b), we have verified that the highest momentum components do not have time enough to smear out the

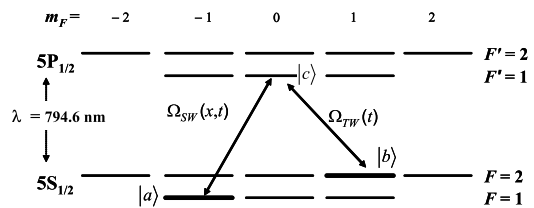


FIG. 4: Hyperfine structure of the D1 transition line of  $^{87}\text{Rb}$  with the couplings  $\Omega_{SW}(x, t)$  and  $\Omega_{TW}(t)$  defining the  $\Lambda$ -scheme. The broader lines correspond to the two condensed trapped states  $|a\rangle = |F = 1, m_F = -1\rangle$  and  $|b\rangle = |F = 2, m_F = 1\rangle$ .

localized structure until the end of the SW where the substrate is placed.

As a second implementation, we now focus on a trapped BEC of  $^{87}\text{Rb}$  to show the feasibility to generate narrow structures in the condensate by means of the SLAP technique. The  $\Lambda$ -type three level configuration under study is depicted in Fig. 4. We consider a zero temperature two-species  $^{87}\text{Rb}$  BEC,  $|a\rangle = |F = 1, m_F = -1\rangle$  and  $|b\rangle = |F = 2, m_F = 1\rangle$ , confined in a one dimensional geometry. The description of the system is performed within the 1D coupled Gross-Pitaevskii equations:

$$i\hbar \frac{d\psi_a}{dt} = \left[ -\frac{\hbar^2}{2m} \Delta + V_a(x) + g_{aa}|\psi_a|^2 + g_{ab}|\psi_b|^2 \right] \psi_a + \frac{1}{2} \hbar \Omega_{SW}(x, t) \psi_c \quad (4)$$

$$i\hbar \frac{d\psi_b}{dt} = \left[ -\frac{\hbar^2}{2m} \Delta + V_b(x) + g_{bb}|\psi_b|^2 + g_{ab}|\psi_a|^2 \right] \psi_b + \frac{1}{2} \hbar \Omega_{TW}(t) \psi_c + \hbar(\Delta_{SW} - \Delta_{TW}) \psi_b \quad (5)$$

$$i\hbar \frac{d\psi_c}{dt} = \frac{1}{2} \hbar \Omega_{SW}(x, t) \psi_a + \frac{1}{2} \hbar \Omega_{TW}(t) \psi_b - i \frac{\Gamma}{2} \psi_c + \hbar \Delta_{SW} \psi_c \quad (6)$$

where the effective 1D nonlinearity is given by  $g_{ij} = 2\hbar a_{ij} \omega_t$ ,  $i, j = a, b$  with  $a_{ij}$  the interspecies ( $i \neq j$ ) and intraspecies ( $i = j$ )  $s$ -wave scattering lengths, and  $\omega_t$  the transverse trapping frequency. In  $^{87}\text{Rb}$  the scattering lengths are known to be in the proportion  $a_{aa} : a_{ab} : a_{bb} = 1.03 : 1 : 0.97$  with the average of the three being  $55(3) \text{ \AA}$  [20]. Since the magnetic moments of the two trapped components are the same to first order, magnetic trapping as well as optical trapping is possible with equal potentials for both components. The axial trapping potential reads  $V_a(x) = V_b(x) = m\omega_x^2 x^2/2$ , with  $m$  the  $^{87}\text{Rb}$  mass and  $\omega_x$  the axial trapping frequency. State  $|c\rangle = |F' = 1, m_F = 0\rangle$  is not trapped and the excited atoms are assumed to escape from the BEC at a rate  $\Gamma = 2\pi \times 5.41 \cdot 10^6 \text{ s}^{-1}$ .

To show the time evolution of the system during the SLAP process, we have numerically solved Eqs. (4)-(6) for a BEC of  $5 \times 10^4$  atoms. Figs. 5(a) and (b) show the mixing angle  $\theta$  at one of the SW anti-nodes and the

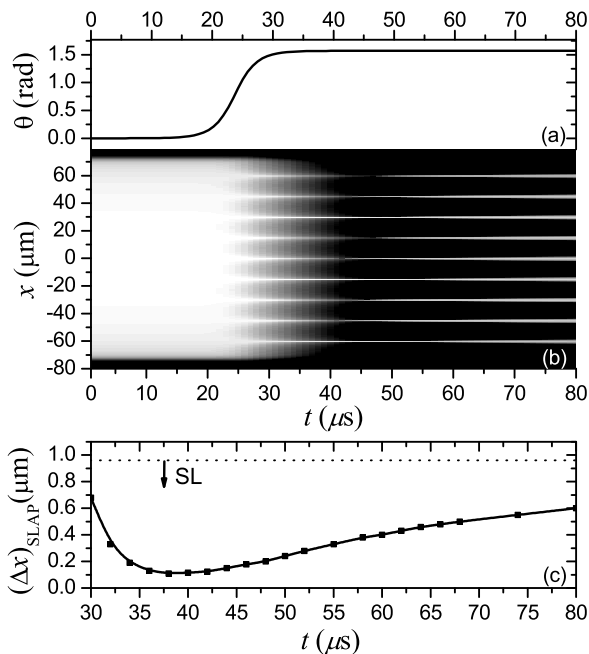


FIG. 5: SLAP technique for a  $^{87}\text{Rb}$  BEC: (a) Time evolution of the mixing angle  $\theta$  at one of the SW anti-nodes. (b) Contour plot of the density distribution of atoms in state  $|a\rangle$  as a function of time during the SLAP technique for a SW with  $15\ \mu\text{m}$  period,  $\mathcal{R} = 100$ ,  $\Omega_{TW0} = 2\pi \times 10 \cdot 10^6\text{s}^{-1}$ ,  $\sigma_{TW} = \sigma_{SW} = 8\ \mu\text{s}$ ,  $t_{TW} = 22\ \mu\text{s}$ ,  $t_{SW} = 36\ \mu\text{s}$ ,  $\Delta_{TW} = \Delta_{SW} = 0$ ,  $\omega_x = 2\pi \times 14\text{s}^{-1}$ , and  $\omega_t = 2\pi \times 715\text{s}^{-1}$ . (c) Time evolution of the FWHM of the central localized structure.

contour plot of the density distribution of atoms in state  $|a\rangle$ , respectively, as a function of time and for the parameters given in the figure caption. As expected, component  $|a\rangle$  develops extremely narrow structures at the nodes of the SW whose width is much smaller than its spa-

tial period. For demonstration, we have chosen a large spatial period of  $15\ \mu\text{m}$  but arbitrary periods down to  $\lambda_{SW}/2$  with a corresponding localization periods down to the nm scale could be achieved by changing the wave number  $k$  of the standing wave. Fig. 5(c) shows the time evolution of the FWHM around one node. The minimal width of the localized structures coincides approximately with the time at which the TW field is switched off, i.e., at  $\theta = \pi/2$ . We have calculated the transverse momentum spread  $\Delta p_x$  for this time, obtaining a beam quality factor [21]  $M^2 = (2/\hbar)\Delta x\Delta p_x \approx 0.6$  which is below the Heisenberg limit due to the non-linearities of the two-component trapped BEC partially compensating for diffraction.

In conclusion, we have introduced the SLAP technique for state-selective localization, patterning, and addressing of atomic matter waves. We have shown that a 'super-localization' regime beating the previously introduced CPT localization technique [6] can be reached and have given analytic expressions for the necessary conditions. Since localization occurs at the nodes of one of the involved laser fields, more evolved patterning schemes can be realized by extending the present 1D configuration to higher dimensions by applying 2D and 3D SW configurations. Even more complex structures, such as the intensity nodes of higher-order Laguerre-Gauss modes or the light fields of custom-made micro-optical elements [22], could be considered for this technique.

We acknowledge support by the Spanish Ministry of Education and Science under contracts FIS2005-01497, FIS2005-01369, HA2005-0002, CSD2006-00019 and the Catalan Government under contract SGR2005-00358, by ESF and DFG under the project CIGMA, by the European Commission within the RTN Atom Chips and the IP SCALA, and by NIST under award 60NANB5D120.

- 
- [1] For a review see: I. Bloch, *Nature Physics* **1**, 23 (2005); M. Lewenstein *et al.*, *Advances in Physics* **56** (2), 243 (2007).
- [2] C. A. Mack, *Fundamental Principles of Optical Lithography: the Science of Microfabrication*, (Chichester, West Sussex, England: Wiley, 2007); M. K. Oberthaler and T. Pfau, *J. Phys.: Condens. Matter* **15**, R233 (2003); J. H. Thywissen and M. Prentiss, *New Journal of Physics* **7**, 47 (2005); D. Meschede and H. Metcalf, *J. Phys. D: Appl. Phys.* **36**, R17 (2003).
- [3] M. Holland *et al.*, *Phys. Rev. Lett.* **76**, 3683 (1996).
- [4] E. Paspalakis and P. L. Knight, *Phys. Rev. A* **63**, 065802 (2001).
- [5] M. Sahrar *et al.*, *Phys. Rev. A* **72**, 013820 (2005).
- [6] G. S. Agarwal, K. T. Kapale, *J. Phys. B: At. Mol. Opt. Phys.* **39**, 3437 (2006).
- [7] J. Cho, *Phys. Rev. Lett.* **99**, 020502 (2007).
- [8] A. V. Gorshkov *et al.*, *Phys. Rev. Lett.* **100**, 093005 (2008).
- [9] S. E. Harris, *Phys. Today* **50**, 36 (1997); E. Arimondo, in *Progress in Optics* edited by E. Wolf, Vol. XXXV, p. 257 (Elsevier Science, Amsterdam, 1996); M. O. Scully and M. S. Zubairy, *Quantum Optics*, Cambridge University Press, England, (1997); J. P. Marangos, *J. Mod. Opt.* **45**, 471 (1998); J. Mompart and R. Corbalán, *J. Opt. B* **2**, R7-R24 (2000); F. Silva *et al.*, *Phys. Rev. A* **64**, 033802 (2001).
- [10] H. Li *et al.*, *Phys. Rev. A* **78**, 013803 (2008).
- [11] K. Bergmann, H. Theuer, and B. W. Shore, *Rev. Mod. Phys.* **70**, 1003 (1998).
- [12] J. R. Kuklinski *et al.*, *Phys. Rev. A* **40**, 6741-6744 (1989).
- [13] See Pierre Meystre, *Atom Optics*, Springer (2001) and reference therein.
- [14] A. Vardi *et al.*, *J. Chem. Phys.* **107**, 6166 (1997); P. S. Julienne *et al.*, *Phys. Rev. A* **58**, R797 (1998); M. Mackie, R. Kowalski and J. Javanainen, *Phys. Rev. Lett.* **84**, 3803 (2000); J. J. Hope, M. K. Olsen, and L. I. Plimak, *Phys. Rev. A* **63**, 043603 (2001); P. D. Drummond *et al.*, *Phys. Rev. A* **65**, 063619 (2002); H. Y. Ling, H. Pu and B. Seaman, *Phys. Rev. Lett.* **93**,

- 250403 (2004); J. Cheng, S. Han and Y. J. Yan, Phys. Rev. A **73**, 035601 (2006).
- [15] K. Winkler *et al.*, Phys. Rev. Lett. **95**, 063202 (2005).
- [16] K. C. Wright, L. S. Leslie and N. P. Bigelow, Phys. Rev. A **77**, 041601(R) (2008).
- [17] P. Engels *et al.*, Appl. Phys. B **69**, 407-412 (1999).
- [18] J. Martin, B. W. Shore, and K. Bergmann, Phys. Rev. A **54**, 1556 (1996).
- [19] M. Zinner *et al.*, Phys. Rev. A **67**, 010501(R) (2003).
- [20] J. M. Vogels *et al.*, Phys. Rev. A **56**, R1067 (1997); M. R. Matthews *et al.*, Phys. Rev. Lett. **81**, 243 (1998).
- [21] J.-F. Riou *et al.*, Phys. Rev. Lett. **96**, 070404 (2006); A. E. Siegman, IEEE J. Quantum Electron. **27**, 1146 (1991); M. Jeppesen *et al.*, Phys. Rev. A **77**, 063618 (2008).
- [22] G. Birkl *et al.*, Opt. Comm. **191**, 67 (2001).